

# Application News No. **P104** **i266**

## EPMA-8050G Electron Probe Microanalyzer High-Speed Impact Testing Machine

### Evaluation of Mechanical Characteristics and Fracture Surface Observation in Static and High-Speed Tensile Tests of Plastic Materials

In recent years, plastic materials have been used in various industrial fields and applications ranging from small gears to automobiles and aircraft, taking advantage of the thermal characteristics and light weight of plastics. These materials may be subjected to dynamic deformation, for example, in collisions involving transportation equipment and when products are dropped. Therefore, in addition to the conventional static testing, impact testing is necessary in order to ensure reliability. In particular, because the polymers that make up plastics display a viscoelastic property, having both viscosity and elasticity, their mechanical characteristics show dependency on the environmental temperature, time, and deformation rate <sup>(1)</sup>.

On the other hand, when damages/failure accidents or deterioration phenomenon occur, investigation and countermeasures are urgently required. Failure of plastics takes a variety of forms, including static fracture, impact fracture, fatigue fracture, creep fracture, fracture due to environmental factors, and fracture due to deterioration, and fracture surfaces with distinctive features can be observed, depending on these various types of fracture <sup>(2)</sup>. This suggests the possibility that the cause of damage can be designated and solutions to the cause can be studied by fracture surface observation.

In this study, the test speed dependencies of an acrylic resin (PMMA) and polypropylene (PP) were evaluated by using a Shimadzu AG-Xplus autograph precision universal testing machine and a HITS-TX high-speed impact testing machine. In addition, the fracture surfaces of the test pieces after tests under various conditions were observed with a Shimadzu EPMA (EPMA-8050G, hereinafter, EPMA) electron probe microanalyzer.

T. Ono, F. Yano, K. Kawane

#### Test Speed Dependency Evaluation System

The AG-Xplus autograph precision universal testing machine was used in static tensile tests, and the HITS-TX was used in high-speed tensile tests. Fig. 1 shows the condition of tests. Table 1 shows the test equipment used in this study. After the tests, the fracture surfaces were coated with gold and observed with an optical microscope and EPMA. Fig. 2 shows the appearance of the EPMA.

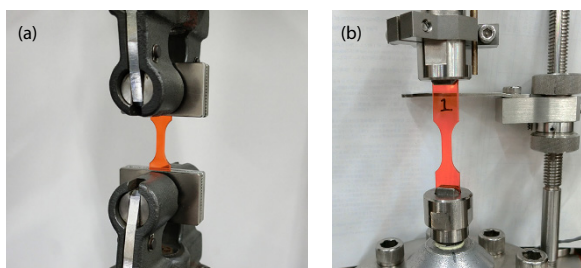


**Fig. 1 Condition of Tests**  
(a) Static Tensile Test (b) High-Speed Tensile Test

**Table 1 Test Equipment**

Testing machine	: AG-Xplus (static tensile test) HITS-TX (high-speed tensile test)
Load cell	: 10 kN
Grip	: Pneumatic parallel grippers (static tensile test) Flat grip (high-speed tensile test)



**Fig. 2 Appearance of EPMA (EPMA-8050G)**

#### Test Results

Tensile tests were conducted with PMMA and PP test pieces. In the static tensile tests, the test speed was set to 5 mm/min for PMMA and 1000 mm/min for PP. In the high-speed tensile tests, the test speed was set to 10 m/sec for both materials. Table 2 shows the test conditions.

The stress-stroke curves and test results are shown in Fig. 3 and Table 3, respectively. The tensile strengths of both PMMA and PP were higher in the high-speed tensile test than in the static tensile test, confirming the test speed dependency of the tensile strength of these two plastic materials.

**Table 2 Test Conditions**

Test speed	: 5 mm/min (PMMA, static tensile test) 1000 mm/min (PP, static tensile test) 10 m/SEC (high-speed tensile test)
Test pieces	: PPMA (width: 5 mm, thickness: 2 mm) PP (width: 3 mm, thickness: 3 mm)

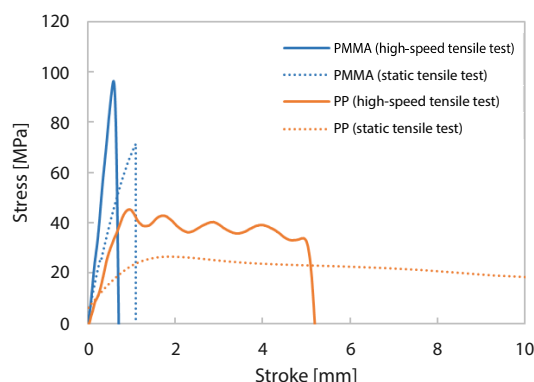


**Fig. 3 Stress-Stroke Curves**

**Table 3 Test Results**

Test piece	Tensile strength [MPa]
PMMA (high-speed tensile test)	96.2
PMMA (static tensile test)	71.3
PP (high-speed tensile test)	45.5
PP (static tensile test)	26.4

## ■ Fracture Surface Observation of PMMA

After the tensile tests, the fracture surfaces of the PMMA samples were coated with gold and observed with an optical microscope and EPMA. The fracture surface of PMMA after the static tensile test is shown in Fig. 4, and that after the high-speed tensile test is shown in Fig. 5. In these figures, (a) shows the optical microscope image and (b) to (l) show the secondary electron images by EPMA.

Looking at the fracture surface from the static tensile test (Fig. 4 (a)), it is estimated that the crack initiated on the left edge and grew toward the right. The EPMA secondary electron images of the left edge, center, and right edge in Fig. 4 (a) are shown in Fig. 4 (b) to (d), respectively. On the left side (Fig. 4 (b)), which is the presumed point of crack initiation, a smooth surface with no distinctive features can be observed. As the crack propagates, a parabolic pattern which was drawn in the direction of crack growth can be observed, as shown in Fig. 4 (e) and its enlarged view in Fig. 4 (i), and with further propagation, an equiaxed parabolic pattern can be observed, as shown in Fig. 4 (f) and its enlargement in Fig. 4 (j). This parabolic pattern is considered to be caused by subcracks that nucleate from impurities or other features of the resin in front of the propagating main crack<sup>(3)</sup>. It is thought that the shape of the parabolic pattern changes due to acceleration of the main crack. Although the equiaxed parabolic pattern could be observed even around the center of the fracture surface, as shown in Fig. 4 (g) and its enlargement in Fig. 4 (k), the morphology of the fracture surface becomes block-like with large differences in level in comparison with the left side in the macro view in Fig. 4 (c). Based on this change in the fracture surface morphology, it is thought that a further acceleration of the crack propagation occurred.

On the other hand, even in the fracture surface (Fig. 5) in the high-speed tensile test, a parabolic pattern (Fig. 5 (e) and its enlargement Fig. 5 (i)) that was drawn in the direction of crack propagation and an equiaxed parabolic pattern (Fig. 5 (f) and its enlargement Fig. 5 (j)) like those in the static tensile test were observed in the upper left part of the fracture surface, which was the presumed point of crack initiation. However, based on the fact that this region is comparatively narrow, it can be inferred that acceleration of the crack occurred quickly after crack initiation. Moreover, in the area around the center of the fracture surface, a block-like fracture surface (Fig. 5 (g)) like that in the static tensile test was observed, and the equiaxed parabolic pattern (Fig. 5 (k)) was also observed.

Finally, focusing on the final fracture part of both fracture surfaces, comparatively smooth parabolic patterns could be confirmed in both specimens. In Fig. 5 (h) and its enlargement Fig. 5 (l), a parabolic pattern which was drawn in the direction of crack growth can be also observed, but at final fracture, the pattern is different from that until that time, suggesting the possibility of deceleration of the crack propagation rate.

## ■ Fracture Surface Observation of PP

As with the PMMA test pieces, after the tests, the surfaces of the PP fracture surfaces were coated with gold and observed with an optical microscope and EPMA. The PP fracture surfaces after the static tensile test and high-speed tensile test are shown in Fig. 6 and Fig. 7, respectively. In these two figures, (a) shows the optical microscope images and (b) to (l) show the secondary electron images by EPMA.

Because the area of the fracture surface in the static tensile test was small in comparison with the area in the high-speed tensile test, it can be understood that the fracture in the static tensile test occurred by plastic deformation accompanied by necking. In the central part of the fracture surface in Fig. 6 (b), a fibrous fracture surface elongated in a ductile manner was observed. Fig. 6 (c) and (d) show enlarged secondary electron images of the left side and vicinity of central area of Fig. 6 (b). Looking at Fig. 6 (d) and its enlargements, Fig. 6 (e) to (h), a condition of fibrous elongation of the resin can be seen. On the other hand, an enlarged view of the periphery of the fracture surface in Fig. 6 (c) reveals numerous holes on the fracture surface, as shown in Fig. 6 (i). However, these are thought to be the result of formation of microcavities nucleating from weak points of the resin (e.g. low molecular weight substances) or impurities. With further enlargement (Fig. 6 (j) to (l)), a condition of elongation of the resin could also be observed.

In the high-speed tensile test, necking did not occur in the fractured part, and a flat and coarse flakey pattern was observed in the entire fracture surface. That is, it is considered that brittle fracture without plastic deformation occurred as a result of the increased testing speed. Enlarged views of the center of the fracture surface are shown in Fig. 7 (d) and (e) to (h), and enlarged views of the outer periphery are shown in Fig. 7 (c) and (i) to (l). No large differences were observed between the fracture surface patterns in the central part and at the outer periphery, and a fracture surface having many microcavities was seen in the entire fracture surface. Moreover, areas displaying fibrous elongation of the resin also could be seen locally. Therefore, it is thought that the crack propagated accompanied by plastic deformation at the microscale.

## ■ Conclusion

The tensile strengths of PMMA and PP were measured by using a Shimadzu AG-Xplus autograph precision universal testing machine and a HITS-TX high-speed impact testing machine. The test speed dependency of the tensile strengths of both PMMA and PP was confirmed, as the tensile strengths of both materials increased at the higher test speed. The fracture surfaces of both plastic materials were also observed with a Shimadzu EPMA-8050G electron probe microanalyzer. With both plastics, distinctive fracture surfaces were observed in the static tensile test and high-speed tensile test, suggesting the possibility that the cause of damage can be designated by fracture surface observation.

Shimadzu test systems can be useful in more accurate evaluations of safety and reliability and root cause analyses of product damage. Although EPMA is generally a main instrument for elemental analyses of micro regions, use of Shimadzu EPMA-8050G enables highly detailed observation of microstructure in the extreme surface region, like that with FE-SEM, even with plastic materials.

## References

- (1) Hiroo Miyairi, Recent Material Performance and Evaluation Technologies (2014)
- (2) Sakae Fujiki, Toshiya Hagiwara, Fracture of Plastic Materials and Observation of Fracture Surfaces (2015)
- (3) Ikuo Narisawa, Fractography of High Polymer Materials (2011)



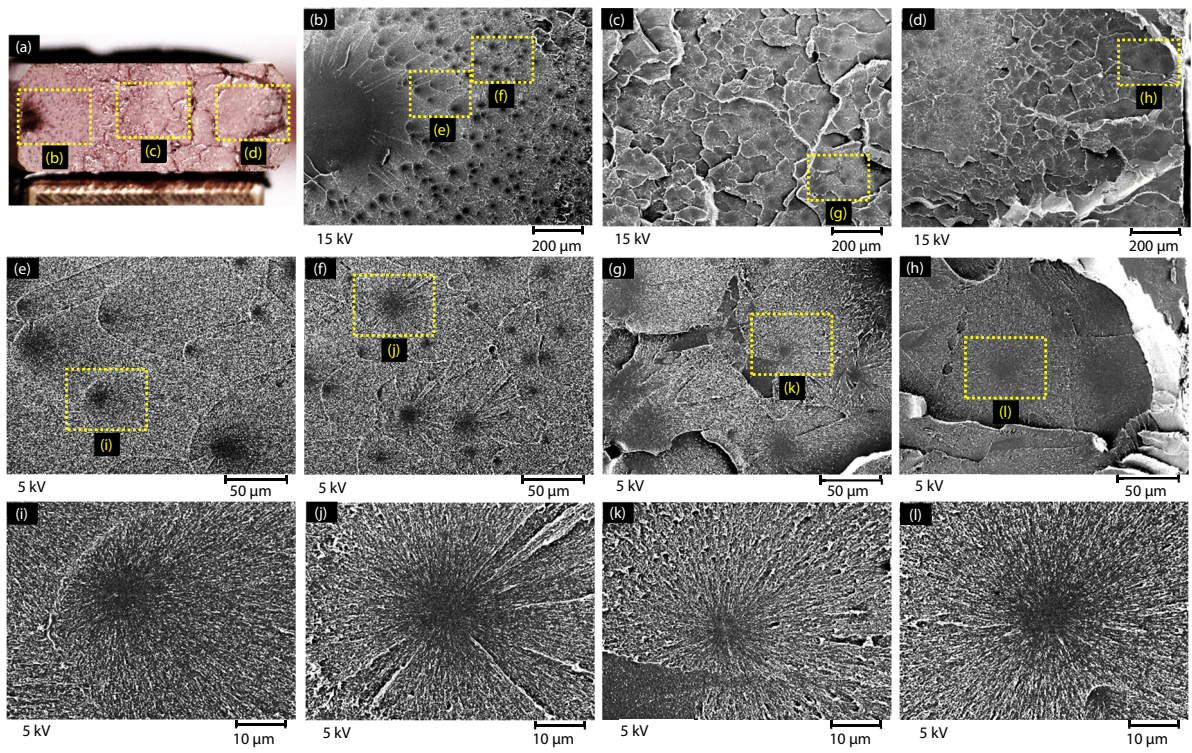


**Fig. 4 Fracture Surface Observation in Static Tensile Test of PMMA**  
(a) Optical Microscope Image, (b) to (l) Secondary Electron Images.

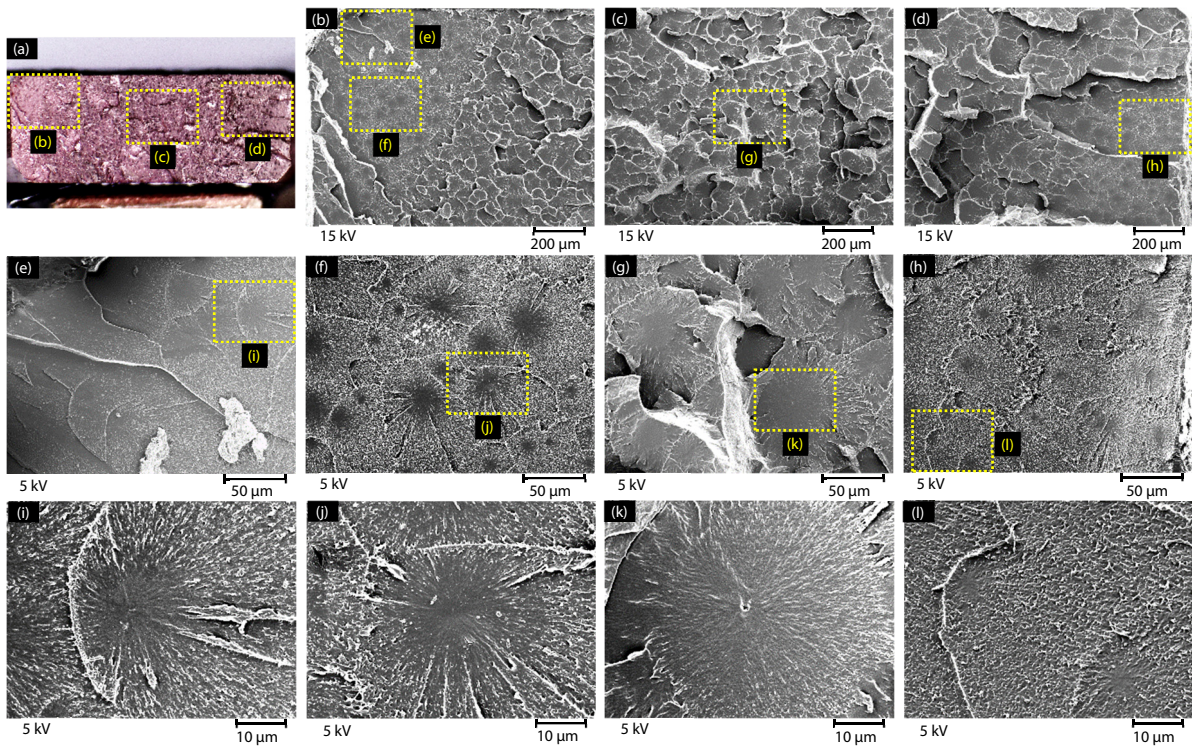


**Fig. 5 Fracture Surface Observation in High-Speed Tensile Test of PMMA**  
(a) Optical Microscope Image, (b) to (l) Secondary Electron Images.



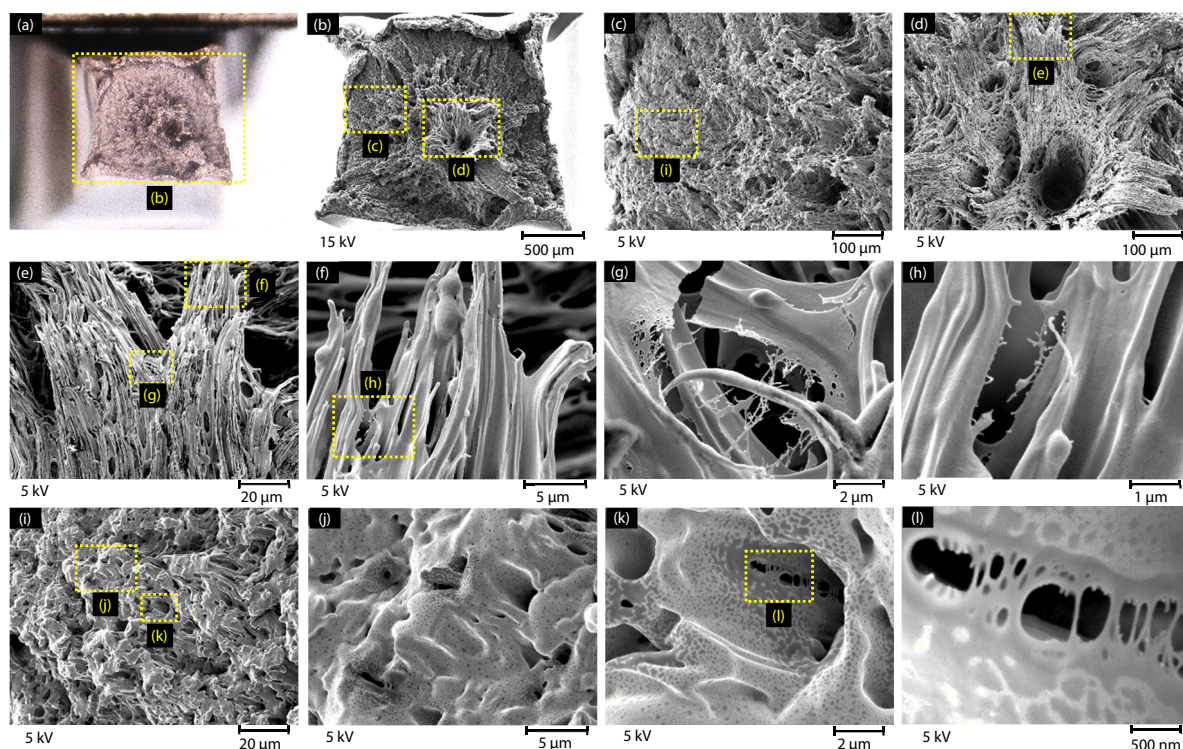


**Fig. 6 Fracture Surface Observation in Static Tensile Test of PP**  
(a) Optical Microscope Image, (b) to (l) Secondary Electron Images.

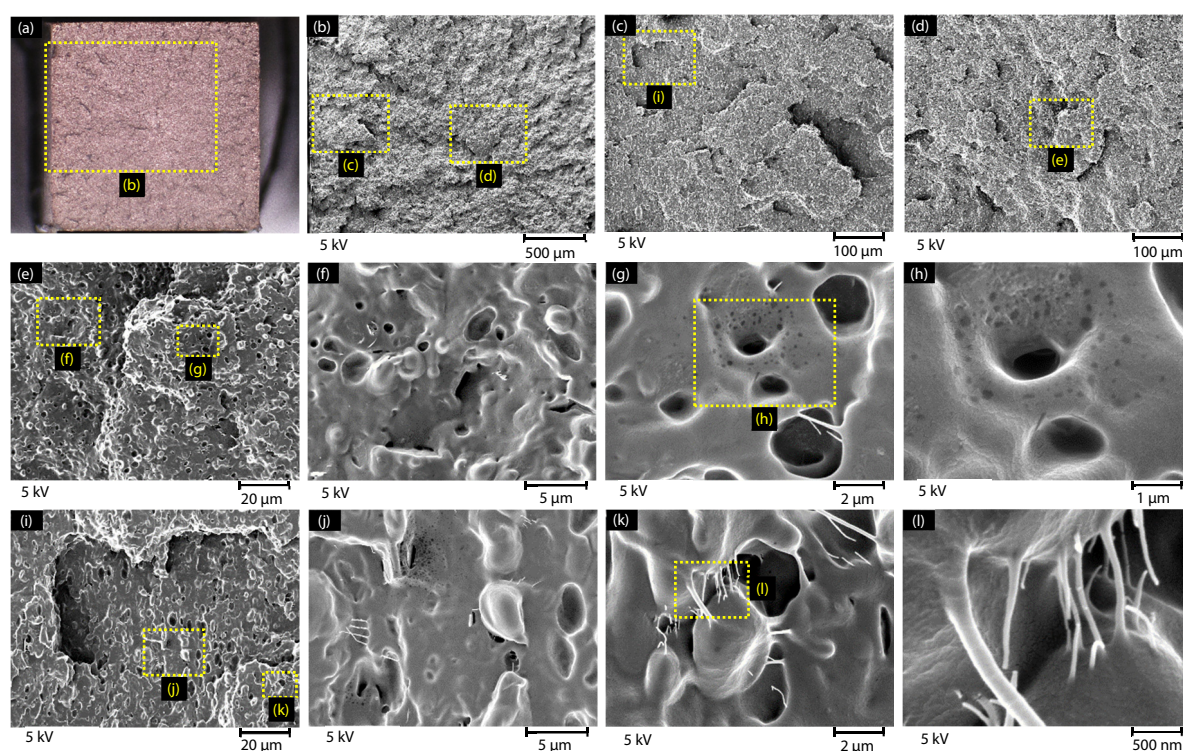


**Fig. 7 Fracture Surface Observation in High-Speed Tensile Test of PP**  
(a) Optical Microscope Image, (b) to (l) Secondary Electron Images.

First Edition: Jan. 2019



Shimadzu Corporation

[www.shimadzu.com/an/](http://www.shimadzu.com/an/)

**For Research Use Only. Not for use in diagnostic procedures.**

This publication may contain references to products that are not available in your country. Please contact us to check the availability of these products in your country.

The content of this publication shall not be reproduced, altered or sold for any commercial purpose without the written approval of Shimadzu. Shimadzu disclaims any proprietary interest in trademarks and trade names used in this publication other than its own. See <http://www.shimadzu.com/about/trademarks/index.html> for details.

The information contained herein is provided to you "as is" without warranty of any kind including without limitation warranties as to its accuracy or completeness. Shimadzu does not assume any responsibility or liability for any damage, whether direct or indirect, relating to the use of this publication. This publication is based upon the information available to Shimadzu on or before the date of publication, and subject to change without notice.

© Shimadzu Corporation, 2019